SCIENCE CHINA
Physics, Mechanics & Astronomy

• Article •

March 2022 Vol. 65 No. 3: 239611
https://doi.org/10.1007/s11433-021-1836-y

Persistent fast kink magnetohydrodynamic waves detected in a quiescent prominence

Dong Li[1,2*], Jianchao Xue[1], Ding Yuan[3*], and Zongjun Ning[1,4]

[1] *Key Laboratory of Dark Matter and Space Astronomy, Purple Mountain Observatory, Chinese Academy of Sciences, Nanjing 210023, China;*
[2] *CAS Key Laboratory of Solar Activity, National Astronomical Observatories, Beijing 100101, China;*
[3] *Institute of Space Science and Applied Technology, Harbin Institute of Technology, Shenzhen 518055, China;*
[4] *School of Astronomy and Space Science, University of Science and Technology of China, Hefei 230026, China*

Received November 18, 2021; accepted December 15, 2021; published online January 19, 2022

Small-scale, cyclic, transverse motions of plasma threads are usually seen in solar prominences, which are often interpreted as magnetohydrodynamic (MHD) waves. Here, we observed small-scale decayless transverse oscillations in a quiescent prominence, and they appear to be omnipresent. The oscillatory periods of the emission intensity and a proxy for the line-of-sight Doppler shift are about half period of the displacement oscillations. This feature agrees well with the fast kink-mode waves in a flux tube. All the moving threads oscillate transversally spatially in phase and exhibit no significant damping throughout the visible segments, indicating that the fast kink MHD waves are persistently powered and ongoing dissipating energy is transferred to the ambient plasma in the quiet corona. However, our calculations suggest that the energy taken by the fast kink MHD waves alone can not support the coronal heating on the quiet Sun.

the Sun, corona, prominence, magnetohydrodynamic (MHD) waves

PACS number(s): 96.60.-j, 96.60.P-, 96.60.Se, 96.50.Tf

Citation: D. Li, J. Xue, D. Yuan, and Z. Ning, Persistent fast kink magnetohydrodynamic waves detected in a quiescent prominence, Sci. China-Phys. Mech. Astron. **65**, 239611 (2022), https://doi.org/10.1007/s11433-021-1836-y

1 Introduction

Solar prominences are cool and dense elongated plasma structures embedded in the surrounding hot corona above the solar limb. Those dark prominences detected on the solar disk are called solar filaments. Usually, the prominence plasmas are about one hundred times cooler and denser than their surrounding coronal plasmas, which raise an important issue for their origin and stability [1, 2]. As one of the most surprising structures suspended by coronal magnetic fields, solar prominences are often regarded as the source/driver of solar eruptions, especially for the large-scale eruption, such as the solar flare or coronal mass ejection [3, 4]. High-resolution observations suggest that they typically consist of a large number of dynamic thread-like structures [5-10], and such thread-like structures also exist in the galaxy clusters [11]. These dynamic behaviors are often linked to the magnetic activities in the corona [12-16], and are therefore employed to understand the origin and physical properties of solar prominences. According to the relative locations, so-

*Corresponding authors (Dong Li, email: lidong@pmo.ac.cn; Ding Yuan, email: yuanding@hit.edu.cn)

lar prominences are usually divided into active region and quiescent prominences. The active region prominences refer to cooler plasmas suspended above the strong magnetic field region, and they are often highly dynamic and relatively short-lived [6,7]. On the contrary, the quiescent prominences are often seen in the quiet-Sun regions, more frequently at high solar latitudes. They are more stable and usually have a longer lifetime [8, 10, 15].

Prominences often show oscillatory motions with a wide range of periods from several minutes to tens of minutes and even several hours, which have been confirmed by the ground- and space-based observations [17-21]. According to the oscillation amplitude, prominence oscillations can be classified as large-scale or small-scale [22]. The large-scale prominence oscillation could disturb a large volume of the whole prominence. This motion is often triggered by the external disturbances, such as Moreton waves or Extreme ultraviolet (EUV) waves, solar flares, and jets [23-25]. The small-scale prominence oscillation is usually detected as the oscillatory motion of a fine thread. It only affects a small part of the prominence. The prominence oscillation could be regarded as a self-oscillation of the coronal plasma structure [8, 26-28], or it may represent a magnetohydrodynamic (MHD) wave mode [6, 7, 29, 30] that reveals the local magnetic nature. The interactions between the fluid motion and magnetic field convert the dynamic energy into smaller length scales, and fine magnetic dynamics could even dissipate the energy into kinetic scales, which are the very nature of MHD waves. On the other hand, the MHD waves are much more general than the wave-guiding effect, and they may carry enough energies which could be converted into heat. Thus, the MHD waves are regarded as a potential source for the plasma heating on the Sun or the Sun-like stars [2, 31-33].

A number of papers reported small-scale transverse oscillations in the plasma threads of solar prominences [6, 27, 30, 34]. Those transverse MHD waves are thought to be driven in the photosphere and propagate upwards along the magnetic field line into the prominence embedded in the corona [32, 35]. The transverse oscillation with the same phase was observed in the moving thread of an active region prominence [6]. However, they failed in determining the exact oscillatory mode, largely due to the absence of line-of-sight (LOS) Doppler velocity measurements. In this paper, we identify that the fast kink mode waves should be responsible for those small-scale transverse oscillations in a quiescent prominence, based on the Hα and its LOS velocity measurements from the New Vacuum Solar Telescope (NVST) [36, 37].

2 Observations

On 08 December 2016, the NVST captured a sequence of high-resolution images of a quiescent prominence above the north-west solar limb, i.e., N21W89. The recording lasted for about 4.5 h, ranging from 04:00 UT to 08:31 UT. The observed data can be accessed at the NVST website http://fso.ynao.ac.cn/cn/datashow.aspx. The Hα images at wavelengths of 6562.8 Å and its two off-bands at ±0.3 Å are used in this study. And the level-1 images are used, which are reconstructed by the frame selection from a large number of raw images by the NVST team [36, 37]. They have a spatial scale of about 0.165 arcsec per pixel, and a time cadence of about 40 s at each bandpass. The data of the Atmospheric Imaging Assembly aboard the Solar Dynamics Observatory (SDO/AIA) at the wavelength of 193 Å are also used here, which have been calibrated with the standard routines in the Solar SoftWare package [38]. It has a time cadence of 12 s, and each pixel corresponds to 0.6 arcsec. It is mainly used to refer the accurate location of the quiescent prominence.

In this study, the ground-based NVST images at different wavebands are co-aligned by the local cross-correlation technique using the FLCA code[1)] [39], which is an efficient method based on the Fourier local correlation tracking [40]. The co-alignment between three NVST wavebands were done by referencing to the AIA 193 Å images. Here, the NVST Hα images at the different bands can be aligned as precise as one pixel. Therefore, the LOS velocity measurement is derived directly from two nearly simultaneous NVST Hα off-band images at two extended wings [27, 37], i.e., ±0.3 Å. Noting that the LOS velocity is a qualitative description rather than a quantitative calculation, it is not the speed value of Doppler shifts.

Figure 1 shows a bright quiescent prominence suspended above the solar limb in Hα line center (a), and two extended wings at ±0.3 Å ((b), (c)), respectively. The quiescent prominence consists of two bright barbs that are connected by a great number of thread-like structures as seen in the NVST Hα images. The prominence threads are very thin, similar to the moving threads seen in the Ca II H line measured by the Hinode/SOT [6]. On the other hand, the double bright barbs are perpendicular to the solar limb, and they are darker than the surrounding corona in AIA 193 Å due to the continuum photoionization, as shown in Figure 1(d). It should be pointed out that the solar prominence has been rotated in Figure 1, so that the moving threads are horizontal. We cannot find the fine-scale threads in AIA 193 Å, largely due to its low spatial resolution. The NVST animation (see Supporting Information, Movie S1, mp4) reveals continuous horizontal

1) https://github.com/xuejcak/flca

motions nearly parallel to the solar limb between two bright barbs of the prominence. These moving threads appear to undergo oscillatory motions in the plane-of-the-sky, which is mainly perpendicular to the moving threads. To investigate the small-scale transverse oscillatory motions in the quiescent prominence, we choose six isolated moving threads that are almost parallel to the solar surface, the thread positions are marked by the short lines in Figure 1(a).

3 Data reductions and results

In order to measure the oscillatory periods and amplitudes of these transverse motions in the moving threads, we first select a crosscut slit that is placed perpendicular to the axis of one moving thread, and then the time-distance plot is constructed along the fixed cut slit. Next, the brightest pixels along the transverse oscillation are selected manually. Finally, a sine function with a linear background (i.e., eq. (1)) is applied to fit the transverse oscillation.

$$A(t) = A_m \sin\left(\frac{2\pi}{P}\, t + \psi\right) + kt + A_0, \tag{1}$$

where A_m represents the displacement amplitude of the transverse oscillation and P is the oscillatory period. While ψ is the initial phase of the oscillatory motion, A_0 represents the position around which the plasma thread oscillates, and k is the drifting velocity in the plane-of-the-sky [25,27]. With the derivative of eq. (1) we can get the velocity amplitude, i.e., $v = 2\pi A_m/P$, as ref. [30].

Figure 2(a)-(d) draw the time-distance images along the moving threads 1 and 2 in the Hα bandpass and its line-of-sight (LOS) velocity, both threads show small-scale displacement oscillations for at least one cycle. Their oscillation amplitudes are estimated to be around 420 and 410 km without any significant damping, and the periods are about 11.0 and 12.0 min, respectively. Table 1 also presents the velocity amplitude (v) of each sample measurement. Figure 2(c) and (d) show that the oscillatory motions tend to be blue-shifted and they reach the maximum (i.e., dashed curves) a bit earlier. Here, the time delay between the Hα line center and LOS velocity are obtained by shifting the fit function with time through the cross-correlation analysis, as shown by the dashed and solid magenta lines. The phase shift is the time lag between the transverse displacement of the oscillating thread in the plane-of-the-sky and the LOS Doppler shift oscillatory signal, but it is normalized to the oscillation period. The short time delay suggests a small phase shift of the transverse oscillation between the Hα line center and its LOS velocity.

To quantify the displacement oscillations of the prominence fine threads, we extract the raw time series from the oscillatory positions (blue pluses) for the Hα emission intensity and the LOS velocity, and then obtain the trend time series with a smooth window of about 20 min. At last, the

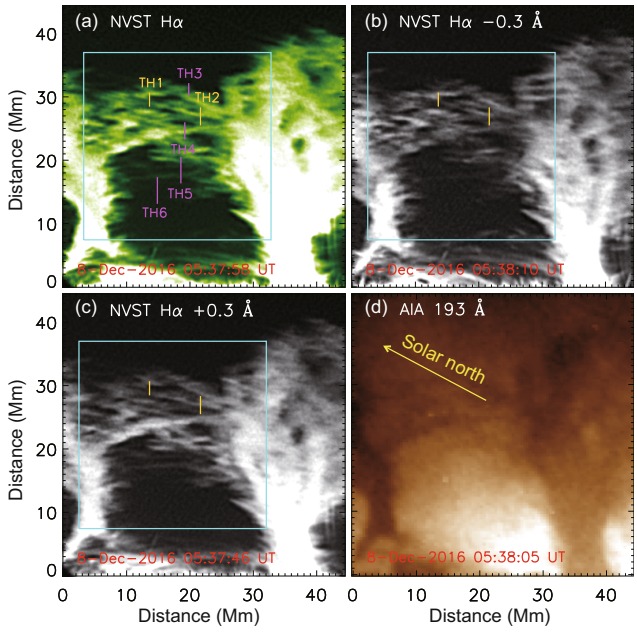

Figure 1 (Color online) Overview of the quiescent prominence on 08 December 2016. Field-of-view measured in NVST Hα at the line center (a), and two extended wings at ±0.3 Å ((b), (c)), and AIA 193 Å (d). The short vertical lines indicate the positions of moving threads of interest, and gold lines are shown in the main text, while the magenta lines are displayed in the Appendix A1 figures. The cyan box marks the region used to perform the animation. The yellow arrow in panel (d) indicates the solar north.

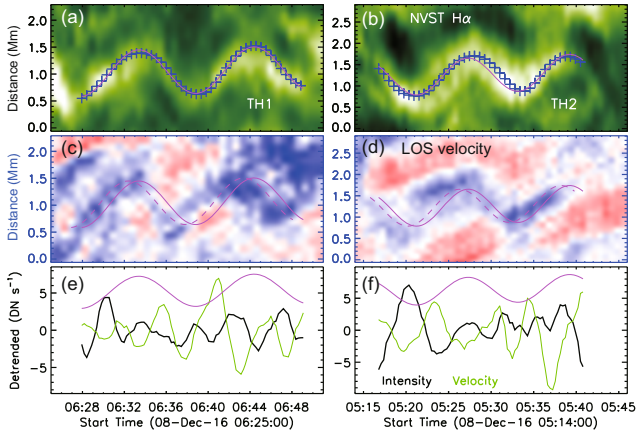

Figure 2 (Color online) (a), (b) Time-distance images taken in the NVST Hα bandpass along the perpendicular slits marked by two gold lines in Figure 1. The blue pluses ("+") mark the bright pixels of the oscillating threads, whereas the continuous magenta line draws a sinusoidal fit. (c), (d) Time-distance images taken in the LOS Doppler velocity along the same two cut slits. The dashed magenta line shows the thread motion on LOS velocity observation, for comparison with the fitted motion (continuous magenta line) in (a) and (b). (e), (f) Detrended time series of the emission intensity (black) and Doppler velocity (green) measured afloat on the oscillatory positions ("+").

detrended time series are calculated by subtracting the trended time series from the raw time series. Figure 2(e) and (f) present the quantitative analysis of the Hα emission intensity (black) and Doppler shift (green) measured afloat on the oscillatory positions. We can see at least four peaks in the Lagrangian emission intensity and Doppler shift, which are twice as more than the double peaks of the displacement oscillation during the same time interval. This suggests that the oscillatory periods in the Lagrangian emission intensity and Doppler shift are no more than half period of the displacement oscillations. On the other hand, the NVST Hα animation (Movie S1) suggests that there is not a violent or obvious eruption nearby the moving threads in the quiescent prominence. However, we shall note that it might occur because that the NVST instrument is not sensitive enough to capture the fine-scale eruptive features, which are as small as the NVST observational limitation.

In order to reach the conclusion that each moving thread oscillates transversally with the same phase, a moving thread with several cut slits along its length should be considered, and two such samples are shown in Figures 3 and 4. Figure 3 presents the snapshots and time-distance images of the plasma thread 1 (TH1) along another three different cut slits, for instance, before and after the fixed cut slit. Figure 3(a) and (b) show two snapshots of TH1 in NVST Hα line center at 06:40:50 UT and 06:44:51 UT, respectively. Four cut slits are made along the moving thread and their time-distance images are plotted in Figure 3(c)-(e), as indicated by S1-S4. Note that the cut slit 3 (dashed line) is at the same position as TH1 in Figure 1(a), and the corresponding time-distance image is given in Figure 2(a), where the magenta curve is obtained. The similar displacement oscillation with the same period can be found in these cut slits along the entire length of the moving thread in NVST Hα bandpass, and no apparent time delay is seen among them, suggesting that there is almost no phase shift along the moving thread for the transverse displacement oscillation. Moreover, they all appear to be decayless. The constant-amplitude oscillations mean that the dissipative losses are compensated by the energy supply. Figure 4 shows the snapshots ((a) and (b)) of TH2 at two fixed instances of time and the time-distance image ((c)-(e)) corresponding to three different perpendicular slits. Similar to the transverse oscillation in the moving thread TH1, the displacement oscillation at three positions along the moving thread TH2 also have an identical period, and there is no significant time delay between them, as shown by the magenta curve in Figure 4. All those observational facts suggest that the small-scale transverse oscillations are most likely to be persistent in the quiescent prominence. The supplementary files such as Figures a1-a4 present the other four isolated threads (TH3-TH6) and their transverse displacement oscillations at different cut slits, further confirming our results. That is, the transverse displacement oscillations can be found at any sites along the moving thread with the same period, without

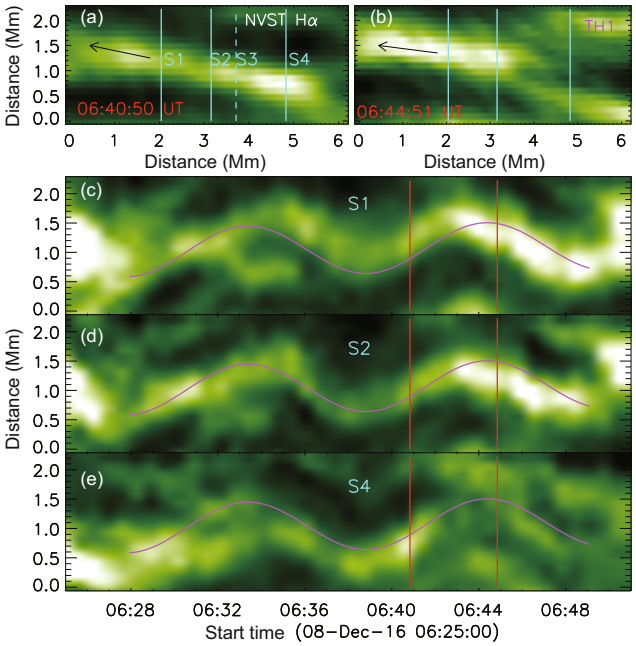

Figure 3 (Color online) Oscillations at multiple positions of the thread TH1. (a), (b) Two snapshots in Hα line center at two fixed instances of time. The vertical cyan lines outline the slit positions, noting that the dashed line corresponds to TH1 in Figure 1, and the arrows indicate the moving direction of the prominence thread. (c)-(e) Time-distance plots corresponding to different perpendicular slits, as marked by the solid cyan lines in (a). Two vertical red lines mark the thread time shown in (a) and (b).

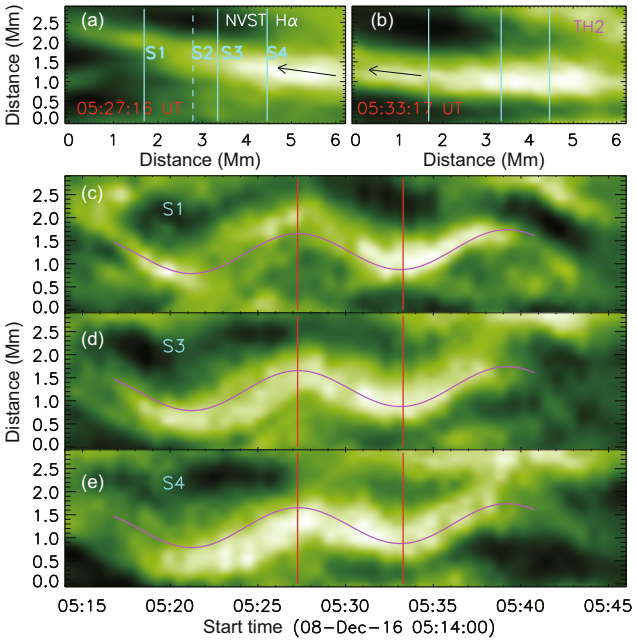

Figure 4 (Color online) Similar to Figure 3 but for the prominence thread TH2.

any significant time delay and damping, implying the omnipresence of small-scale decayless transverse MHD waves.

4 Conclusion and discussion

The small-scale transverse oscillations are largely perpendicular to the moving threads found in the quiescent prominence. Key parameters measured in the six moving threads are summarized in Table 1. The displacement amplitudes range from 420 to 980 km, whereas the respective velocity amplitudes are 4.0 and 6.2 km s^{-1}. The oscillation periods are measured to be about 10.3-16.5 min, these values are larger than those observed in the moving threads of an active region prominence (about 2-4 min) [6], but similar to the case in quiescent prominences [41]. On the other hand, we can not detect any eruptive events near the moving threads during the oscillatory time, suggesting that those small-scale transverse oscillations could be regarded as the self-oscillatory processes of the magnetic structure in the quiescent prominence [8, 26-28, 30] rather than being induced by external disturbances [23-25]. Recent study [42] found that the random motion could excite decayless transverse oscillations in coronal loops, which might be used to explain the excitation of transverse oscillatory motions seen in the quiescent prominence, since such a behavior appears without apparent impulsive energy release or periodic driving.

An intriguing feature is that the transverse displacement oscillations measured at any positions are mostly perpendicular to the moving threads, there is no apparent time delay in different cut slits along the entire length of each moving thread. That is, the transverse oscillation appears to oscillate synchronously along the entire length of each moving thread. It seems that the transverse oscillations always exist (or persist) in the quiescent prominence, when an isolated thread moves to an appropriate position and direction, i.e., the moving thread is largely perpendicular to the oscillation and no other threads or bright patches are mixed with it, then the transverse oscillation can be seen in the plane of the sky. Magnetic fields in the solar/stellar corona are often thought to play a major role in guiding MHD waves. Therefore, the transverse oscillations observed in moving threads of the quiescent prominence are most likely to be regarded as transverse MHD waves in the corona [35], such as fast kink waves [30, 43, 44], or Alfvén waves [32]. The transverse MHD waves are persistent in the quiescent prominence, which are similar to the persistent kink/Alfvén waves observed in coronal loops [45, 46]. The omnipresence of decayless transverse oscillations of coronal loops have also been demonstrated to be a common phenomenon in the solar corona [47], while both the coronal loops and prominence threads could be regarded as the thin magnetic flux tubes in the corona [6, 48, 49]. On the other hand, to maintain the coronal temperature at one million K in the quiet Sun, there should be interplay between continuous cooling and heating processes [50]. Since the small-scale transverse MHD waves are omnipresent in the quiet corona, they could provide ongoing energy input that balances the energy losses in the solar/stellar quiet corona [31, 33, 51].

If we further consider the LOS velocity, the moving threads undergo similar transverse oscillatory motions with a very close period at the blue-shifted wing, and the phase shifts of $\sim\frac{1}{5}\pi$-$\frac{1}{4}\pi$ are detected. Moreover, half period of transverse displacement oscillations can be found in the time series taken from the oscillatory positions at the Hα emission intensity and Doppler shift (Figure 2(e) and (f)), which agrees well with the forward modeling of MHD waves in the fast kink mode of magnetic flux tubes such as prominence fine threads [48, 52] or coronal loops [53, 54]. Therefore, the small-scale transverse oscillations observed in moving threads appear to be more appropriately explained as the fast kink mode waves that propagate along the magnetic field lines in the corona on the quiet Sun, and they might play a certain role in heating the quiet corona [6, 32]. However, it is still unknown if the fast kink MHD waves convey enough energy to heat the quiet corona here.

The kink-like motions in prominence threads have been well documented [21]. The Doppler velocities along a fila-

Table 1 Key parameters measured in six moving threads

Notation	Parameter	TH1	TH2	TH3	TH4	TH5	TH6
Displacement amplitude	A_m (km)	420	450	510	420	980	720
Oscillatory period	P (min)	11.0	12.0	12.1	10.3	16.5	12.6
Velocity amplitude	v (km s^{-1})	4.0	3.9	4.4	4.3	6.2	6.0
Minimum wavelength	$\lambda_{\min}$ ($\times10^3$ km)	109	121	127	106	153	121
Phase speed	$c_{\rm ph}$ (km s^{-1})	165	168	175	172	155	160
Alfvén speed	$V_{\rm A}$ (km s^{-1})	117	119	124	122	110	113
Magnetic field strength	B ($\times10^{-4}$ T)	5.4	5.5	5.7	5.6	5.0	5.2
Magnetic field perturbation	b ($\times10^{-4}$ T)	0.131	0.129	0.144	0.139	0.201	0.195
Energy flux density	$\langle E_k\rangle$ (W m^{-2})	16.7	16.2	21.4	19.9	37.3	36.2

ment thread were found to oscillate with the same phase and period [55], and the Doppler velocities were measured over a rectangular area. Moreover, they [55] reported the longitudinal oscillation along the plasma threads rather than oscillations normal to the magnetic field flux. Using the high spatial resolution observations, the kink-like mode waves were detected as the transverse displacement oscillations along the perpendicular slit in filament/prominence threads, which were excited by EUV waves or solar flares [56, 57]. The kink oscillations were also observed simultaneously along the LOS and in the plane-of-the-sky [7, 30]. Moreover, The small-scale transverse oscillations were seen in an active region prominence, and each moving thread oscillates transversally in phase with the same period [6]. However, authors [6] were not able to determine the exact oscillatory mode, due to the lack of Doppler velocity observations. Later numerical calculations [43] suggested that the kink-mode waves should be responsible for those thread oscillations. In this study, we observed the omnipresence of small-scale transverse oscillations in a quiescent prominence. Each plasma thread shows transverse oscillations with the same phase and period, while the time series of emission intensity and Doppler velocity reveal only half period of the displacement oscillations. All our observational results indicate that the small-scale transverse oscillation could be regarded as the fast kink-mode MHD wave [48, 52-54].

Based on the kink wave model in magnetic flux tube [6, 30, 53, 54, 58], the magnetic field strengths in the quiescent prominence are then estimated to be about 5.0×10^{-4}-5.7×10^{-4} T, which are in accordance with previous findings in fine thread-like structures of solar filament/prominence in the quiet Sun [13, 24, 30]. The Lagrangian perturbations of magnetic fields are also estimated using the Lagrangian displacement vector [53], which are roughly equal to 0.129×10^{-4}-0.201×10^{-4} T. The Alfvén speeds are estimated to be 110-124 km s^{-1}, similar to the measurement (100 km s^{-1}) in quiescent prominences [21]. However, the magnetic field strengths and Alfvén speeds are much smaller than those measured in the moving threads of the active region prominence [6], which are estimated to be roughly 5×10^{-3} T and >1050 km s^{-1}, respectively. We shall note that our measurements are the lower limit estimations using the prominence seismology.

In order to make clear whether the energy taken by the fast kink MHD waves is enough to heat the quiet corona, the time-averaged energy flux density ($\langle E_k \rangle$) [29] for the fast kink MHD waves is then estimated in the quiescent prominence, which is situated in the corona on the quiet Sun, as shown in Table 1. The energy flux densities in the six moving threads are estimated to be about 16.2-37.3 W m^{-2}, which are not sufficient for heating the quiet corona, i.e., 100-200 W m^{-2}, as reported in refs. [59, 60]. It is commonly accepted that the energy flux density calculated by the expression for fast kink MHD waves (i.e., eq. (a4)) could be overestimated [49]. Therefore, the real energy flux taken by the persistent kink MHD wave is not efficient to heat the quiet corona, although they could provide ongoing heating. Our result is consistent with previous findings, for instance, the observed MHD waves do not have enough energy to heat solar active regions [61, 62].

We want to stress that the periods of small-scale transverse motions detected in the quiescent prominence are about 10.3-16.5 min, which are similar to the oscillatory periods of about 5-16 min observed in two quiescent filaments [55]. The similar periods of 3-9 min are also reported in the individual thread of a quiescent filament, which were regarded as the evidence of traveling waves [34]. All those observed periods can be grouped into the short-period (1-20 min) category [17], and they could be regarded as the decayless MHD waves propagating along the fine threads [34]. On the other hand, the animation (Movie S1) shows that the bright barbs undergo large-scale perturbations. However, the period of large-scale perturbations seems to be much larger than those periods of the transverse motions in fine threads. Because the animation (Movie S1) is from about 05:10 UT to 07:50 UT, including all the moving threads in our study, the examined transverse motions are most likely to be the kink-mode MHD waves adhering to individual threads [6, 34] rather than part of the collective behavior of the entire prominence system.

5 Summary

In this study, we report the small-scale transverse oscillatory motions in six moving threads of a quiescent prominence measured by the NVST in Hα and its LOS velocity images. They are identified as the persistent fast kink-mode waves, without significant damping. Our observations indicate that a balance could be maintained between the wave energy dissipation and injection in the quiet corona. However, the wave energy carried by the fast kink MHD waves alone is not sufficient for heating the coronal plasma in the quiet Sun. It is believed the forthcoming 1.8-m telescopes [63] can detect more detailed features of this type of small-scale oscillations in filaments/prominences.

This work was supported by the National Natural Science Foundation of China (Grant Nos. 11973092, 12173012, 12111530078, 12073081, U1631242, 11820101002, 11790302, and U1731241), and the CAS Strategic Priority Research Program on Space Science (Grant Nos. XDA15052200, XDA15320103, and XDA15320301). Dong Li is also supported by the CAS Key Laboratory of Solar Activity (Grant No. KLSA202003), and the Surface Project of Jiangsu Province (Grant No. BK20211402). Ding Yuan is supported by the Shenzhen Technology Project

(Grant No. GXWD20201230155427003-20200804151658001). The Laboratory No. is 2010DP173032. The authors thank the NVST and SDO/AIA teams for providing the data.

Supporting Information

The supporting information is available online at phys.scichina.com and link.springer.com. The supporting materials are published as submitted, without typesetting or editing. The responsibility for scientific accuracy and content remains entirely with the authors.

1 D. H. Mackay, J. T. Karpen, J. L. Ballester, B. Schmieder, and G. Aulanier, Space Sci. Rev. **151**, 333 (2010), arXiv: 1001.1635.
2 S. E. Gibson, Living Rev. Sol. Phys. **15**, 7 (2018).
3 S. Parenti, Living Rev. Sol. Phys. **11**, 1 (2014).
4 P. F. Chen, A. A. Xu, and M. D. Ding, Res. Astron. Astrophys. **20**, 166 (2020), arXiv: 2010.02462.
5 Y. Lin, O. Engvold, L. R. der Voort, J. E. Wiik, and T. E. Berger, Sol. Phys. **226**, 239 (2005).
6 T. J. Okamoto, S. Tsuneta, T. E. Berger, K. Ichimoto, Y. Katsukawa, B. W. Lites, S. Nagata, K. Shibata, T. Shimizu, R. A. Shine, Y. Suematsu, T. D. Tarbell, and A. M. Title, Science **318**, 1577 (2007), arXiv: 0801.1958.
7 T. J. Okamoto, P. Antolin, B. D. Pontieu, H. Uitenbroek, T. V. Doorsselaere, and T. Yokoyama, Astrophys. J. **809**, 71 (2015), arXiv: 1506.08965.
8 Z. Ning, W. Cao, T. J. Okamoto, K. Ichimoto, and Z. Q. Qu, Astron. Astrophys. **499**, 595 (2009).
9 X. L. Yan, Z. K. Xue, Y. Y. Xiang, and L. H. Yang, Res. Astron. Astrophys. **15**, 1725 (2015), arXiv: 1502.03546.
10 Y. Bi, B. Yang, T. Li, Y. Dong, and K. Ji, Astrophys. J. **891**, L40 (2020), arXiv: 2003.08075.
11 Y. H. Zhou, P. F. Chen, J. Hong, and C. Fang, Nat. Astron. **4**, 994 (2020), arXiv: 2104.13564.
12 L. Li, and J. Zhang, Sol. Phys. **282**, 147 (2013).
13 B. Schmieder, T. A. Kucera, K. Knizhnik, M. Luna, A. Lopez-Ariste, and D. Toot, Astrophys. J. **777**, 108 (2013), arXiv: 1309.1568.
14 Z. Ning, W. Cao, and P. R. Goode, Astrophys. J. **707**, 1124 (2009).
15 Y. Shen, Y. Liu, Y. D. Liu, P. F. Chen, J. Su, Z. Xu, and Z. Liu, Astrophys. J. **814**, L17 (2015), arXiv: 1511.02489.
16 Y. Taroyan, and R. Soler, Astron. Astrophys. **631**, A144 (2019).
17 O. Engvold, in *INTAS Workshop on MHD Waves in Astrophysical Plasmas: Proceedings of the INTAS Workshop*, In: J. L. Ballester, and B. Roberts, eds., Universitat de les Illes Balears, Palma de Mallorca, Universitat de les Illes Balears, 2001.
18 C. Foullon, E. Verwichte, and V. M. Nakariakov, Astron. Astrophys. **427**, L5 (2004).
19 G. Pouget, K. Bocchialini, and J. Solomon, Astron. Astrophys. **450**, 1189 (2006).
20 Q. M. Zhang, D. Li, and Z. J. Ning, Astrophys. J. **851**, 47 (2017), arXiv: 1711.00670.
21 I. Arregui, R. Oliver, and J. L. Ballester, Living Rev. Sol. Phys. **15**, 3 (2018).
22 R. Oliver, and J. L. Ballester, Sol. Phys. **206**, 45 (2002).
23 A. Asai, T. T. Ishii, H. Isobe, R. Kitai, K. Ichimoto, S. UeNo, S. Nagata, S. Morita, K. Nishida, D. Shiota, A. Oi, M. Akioka, and K. Shibata, Astrophys. J. **745**, L18 (2012), arXiv: 1112.5915.
24 Y. Shen, K. Ichimoto, T. T. Ishii, Z. Tian, R. Zhao, and K. Shibata, Astrophys. J. **786**, 151 (2014), arXiv: 1403.7705.
25 Q. M. Zhang, J. H. Guo, K. V. Tam, and A. A. Xu, Astron. Astrophys. **635**, A132 (2020), arXiv: 2001.01250.
26 V. M. Nakariakov, S. A. Anfinogentov, G. Nisticò, and D. H. Lee, Astron. Astrophys. **591**, L5 (2016).
27 D. Li, Y. Shen, Z. Ning, Q. Zhang, and T. Zhou, Astrophys. J. **863**, 192 (2018), arXiv: 1807.03942.
28 S. F. Martin, Y. Lin, and O. Engvold, Sol. Phys. **250**, 31 (2008).
29 R. J. Morton, G. Verth, D. B. Jess, D. Kuridze, M. S. Ruderman, M. Mathioudakis, and R. Erdélyi, Nat. Commun. **3**, 1315 (2012), arXiv: 1306.4124.
30 Y. Lin, R. Soler, O. Engvold, J. L. Ballester, Ø. Langangen, R. Oliver, and L. H. M. Rouppe van der Voort, Astrophys. J. **704**, 870 (2009), arXiv: 0909.2792.
31 T. Van Doorsselaere, A. K. Srivastava, P. Antolin, N. Magyar, S. Vasheghani Farahani, H. Tian, D. Kolotkov, L. Ofman, M. Guo, I. Arregui, I. De Moortel, and D. Pascoe, Space Sci. Rev. **216**, 140 (2020), arXiv: 2012.01371.
32 L. Melis, R. Soler, and J. L. Ballester, Astron. Astrophys. **650**, A45 (2021), arXiv: 2103.16599.
33 A. K. Srivastava, J. L. Ballester, P. S. Cally, M. Carlsson, M. Goossens, D. B. Jess, E. Khomenko, M. Mathioudakis, and T. V. Zaqarashvili, J. Geo. Res. **126**, e029097 (2021).
34 Y. Lin, O. Engvold, L. H. M. Rouppe van der Voort, and M. van Noort, Sol. Phys. **246**, 65 (2007).
35 V. M. Nakariakov, and D. Y. Kolotkov, Annu. Rev. Astron. Astrophys. **58**, 441 (2020).
36 Z. Liu, J. Xu, B. Z. Gu, S. Wang, J. Q. You, L. X. Shen, R. W. Lu, Z. Y. Jin, L. F. Chen, K. Lou, Z. Li, G. Q. Liu, Z. Xu, C. H. Rao, Q. Q. Hu, R. F. Li, H. W. Fu, F. Wang, M. X. Bao, M. C. Wu, and B. R. Zhang, Res. Astron. Astrophys. **14**, 705 (2014).
37 X. L. Yan, Z. Liu, J. Zhang, and Z. Xu, Sci. China Tech. Sci. **63**, 1656 (2020), arXiv: 1910.09127.
38 J. R. Lemen, A. M. Title, D. J. Akin, P. F. Boerner, C. Chou, J. F. Drake, D. W. Duncan, C. G. Edwards, F. M. Friedlaender, G. F. Heyman, N. E. Hurlburt, N. L. Katz, G. D. Kushner, M. Levay, R. W. Lindgren, D. P. Mathur, E. L. McFeaters, S. Mitchell, R. A. Rehse, C. J. Schrijver, L. A. Springer, R. A. Stern, T. D. Tarbell, J. P. Wuelser, C. J. Wolfson, C. Yanari, J. A. Bookbinder, P. N. Cheimets, D. Caldwell, E. E. Deluca, R. Gates, L. Golub, S. Park, W. A. Podgorski, R. I. Bush, P. H. Scherrer, M. A. Gummin, P. Smith, G. Auker, P. Jerram, P. Pool, R. Soufli, D. L. Windt, S. Beardsley, M. Clapp, J. Lang, and N. Waltham, Sol. Phys. **275**, 17 (2012).
39 J. C. Xue, J. C. Vial, Y. Su, H. Li, Z. Xu, Y. N. Su, T. H. Zhou, and Z. T. Li, Res. Astron. Astrophys. **21**, 222 (2021).
40 G. H. Fisher, and B. T. Welsch, Subsurf. Atmosph. Influe. Solar Act. **383**, 373 (2008).
41 Y. H. Zhou, C. Xia, R. Keppens, C. Fang, and P. F. Chen, Astrophys. J. **856**, 179 (2018), arXiv: 1803.03385.
42 A. N. Afanasyev, T. Van Doorsselaere, and V. M. Nakariakov, Astron. Astrophys. **633**, L8 (2020), arXiv: 1912.07980.
43 T. Van Doorsselaere, V. M. Nakariakov, and E. Verwichte, Astrophys. J. **676**, L73 (2008).
44 J. Terradas, I. Arregui, R. Oliver, and J. L. Ballester, Astrophys. J. **678**, L153 (2008), arXiv: 0803.2649.
45 H. Tian, S. W. McIntosh, T. Wang, L. Ofman, B. De Pontieu, D. E. Innes, and H. Peter, Astrophys. J. **759**, 144 (2012), arXiv: 1209.5286.
46 S. Anfinogentov, G. Nisticò, and V. M. Nakariakov, Astron. Astrophys. **560**, A107 (2013).
47 S. A. Anfinogentov, V. M. Nakariakov, and G. Nisticò, Astron. Astrophys. **583**, A136 (2015), arXiv: 1509.05519.
48 A. J. Díaz, R. Oliver, R. Erdélyi, and J. L. Ballester, Astron. Astrophys. **379**, 1083 (2001).
49 M. Goossens, T. Van Doorsselaere, R. Soler, and G. Verth, Astrophys. J. **768**, 191 (2013).
50 D. Y. Kolotkov, D. I. Zavershinskii, and V. M. Nakariakov, arXiv: 2111.02370.
51 H. Tian, E. E. DeLuca, S. R. Cranmer, B. De Pontieu, H. Peter, J. Martínez-Sykora, L. Golub, S. McKillop, K. K. Reeves, M. P. Miralles, P. McCauley, S. Saar, P. Testa, M. Weber, N. Murphy, J. Lemen, A. Title, P. Boerner, N. Hurlburt, T. D. Tarbell, J. P. Wuelser, L. Kleint, C. Kankelborg, S. Jaeggli, M. Carlsson, V. Hansteen, and S. W. McIntosh, Science **346**, 1255711 (2014), arXiv: 1410.6143.
52 P. S. Joarder, V. M. Nakariakov, and B. Roberts, Sol. Phys. **173**, 81

(1997).
53 D. Yuan, and T. V. Doorsselaere, Astrophys. J. Suppl. Ser. **223**, 23 (2016), arXiv: 1603.01632.
54 D. Yuan, and T. V. Doorsselaere, Astrophys. J. Suppl. Ser. **223**, 24 (2016), arXiv: 1602.07598.
55 Y. Zhang, O. Engvold, and S. L. Keil, Sol. Phys. **132**, 63 (1991).
56 W. Liu, L. Ofman, N. V. Nitta, M. J. Aschwanden, C. J. Schrijver, A. M. Title, and T. D. Tarbell, Astrophys. J. **753**, 52 (2012), arXiv: 1204.5470.
57 Z. K. Xue, X. L. Yan, Z. Q. Qu, and L. Zhao, in *Transverse oscillation of a filament triggered by an extreme ultraviolet wave: Proceedings of the Solar Polarization 7*, Astronomical Society of the Pacific Conference Series, Kunming, 2013.
58 V. M. Nakariakov, S. A. Anfinogentov, P. Antolin, R. Jain, D. Y. Kolotkov, E. G. Kupriyanova, D. Li, N. Magyar, G. Nisticò, D. J. Pascoe, A. K. Srivastava, J. Terradas, S. Vasheghani Farahani, G. Verth, D. Yuan, and I. V. Zimovets, Space Sci. Rev. **217**, 73 (2021), arXiv: 2109.11220.
59 G. L. Withbroe, and R. W. Noyes, Annu. Rev. Astron. Astrophys. **15**, 363 (1977).
60 M. J. Aschwanden, A. Winebarger, D. Tsiklauri, and H. Peter, Astrophys. J. **659**, 1673 (2007).
61 J. A. Klimchuk, Sol. Phys. **234**, 41 (2006), arXiv: astro-ph/0511841.
62 J. A. Klimchuk, Philosoph. Trans. R. Soc. London Ser. A, **373**, 20140256 (2015).
63 C. H. Rao, N. T. Gu, X. J. Rao, C. Li, L. Q. Zhang, J. L. Huang, L. Kong, M. Zhang, Y. T. Cheng, Y. Pu, H. Bao, Y. M. Guo, Y. Y. Liu, J. S. Yang, L. B. Zhong, C. J. Wang, K. Fang, X. J. Zhang, D. H. Chen, C. Wang, X. L. Fan, Z. W. Yan, K. L. Chen, X. Y. Wei, L. Zhu, H. Liu, Y. J. Wan, H. Xian, and W. L. Ma, Sci. China-Phys. Mech. Astron. **63**, 109631 (2020).

Appendix

A1 Prominence oscillations in other four moving threads

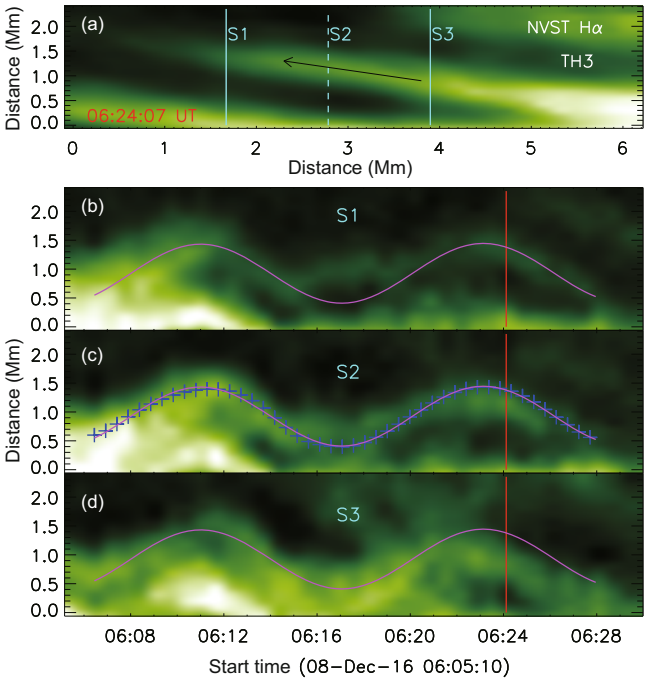

Figure a1 (Color online) Similar to Figure 3 but for the prominence thread TH3.

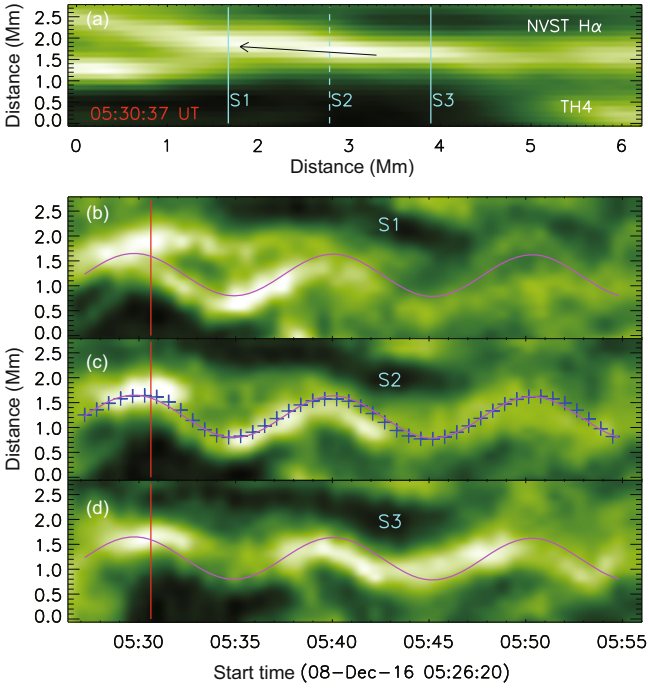

Figure a2 (Color online) Similar to Figure 3 but for the prominence thread TH4.

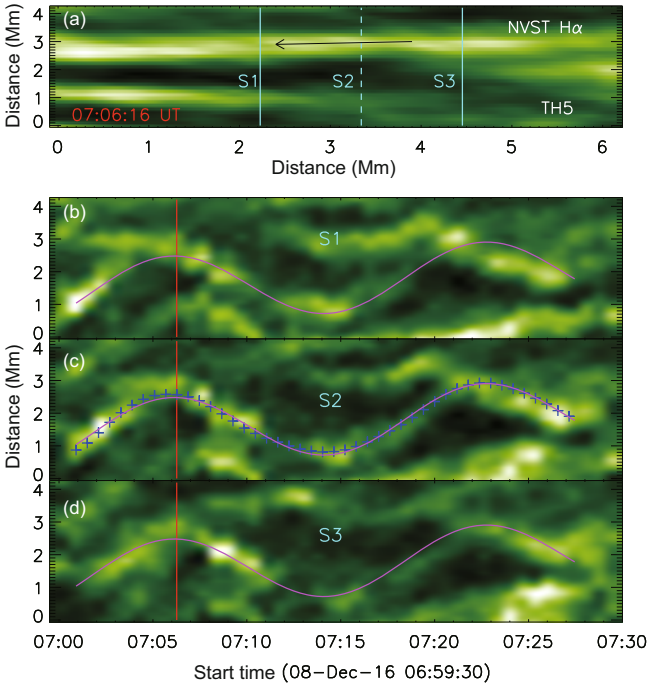

Figure a3 (Color online) Similar to Figure 3 but for the prominence thread TH5.

A2 Prominence seismology

The upper limit of an uncertainty in the phase of the transverse oscillation is estimated to be the ratio of the NVST time

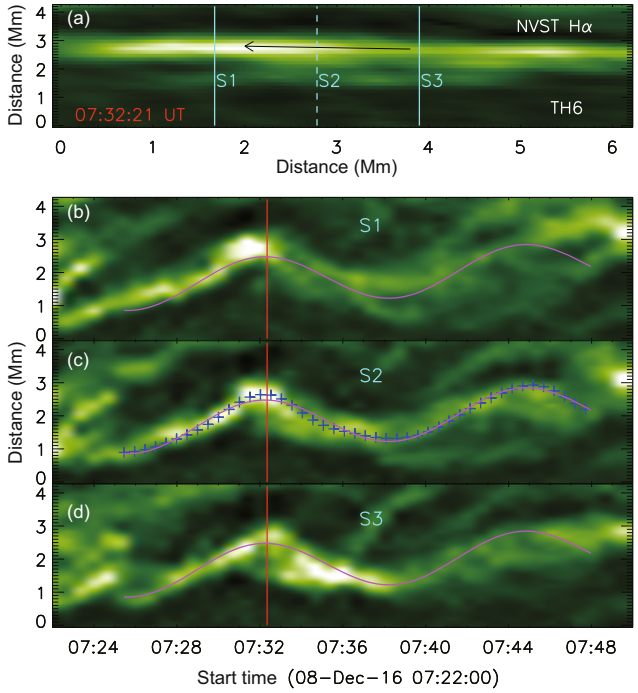

Figure a4 (Color online) Similar to Figure 3 but for the prominence thread TH6.

cadence and the detected oscillatory period (P). This is because we cannot find any significantly phase shift (or time delay) at different cut slit locations along the entire length of each moving thread, suggesting that the time delay is much shorter than the time resolution of the NVST. Then we can deduce the minimum wavelength ($\lambda_{\rm min}$) of the transverse oscillation for a specific oscillatory period (P) in the moving thread. The thread lengths are measured from the Hα images, regarding the lower time resolution (i.e., ~40 s) of the NVST, and the fine-scale thread is moving quickly (see the animation of S1), the thread length measured here is also a lower limit [6].

Next, we can estimate the lower limit of phase/wave speed ($c_{\rm ph}$) by using the relationship between the minimum wavelength and period, i.e., eq. (a1), if we considered the transverse oscillation as the transverse MHD wave in the solar corona [6, 30]. Then, using eqs. (a2) and (a3), the Alfvén speed ($V_{\rm A}$) and the implied magnetic field strength (B) of the transverse MHD wave can also be calculated, basing on the kink model in the solar atmosphere [45, 53, 54].

$$c_{\rm ph} \approx \frac{\lambda_{\rm min}}{P}, \tag{a1}$$

$$V_{\rm A} = \frac{c_{\rm ph}}{\sqrt{2}}, \tag{a2}$$

$$B \approx V_{\rm A}\sqrt{\mu_0 \rho}, \tag{a3}$$

where μ_0 is the magnetic permittivity of free space, which is $\mu_0 = 4\pi \times 10^{-7}$ N A^{-2}. While ρ represents the plasma density in the quiescent prominence. In this study, a relatively low value of the plasma density [6, 30] in the quiescent prominence is used as $\rho = 1.67 \times 10^{-11}$ kg m^{-3} (~10^{10} cm^{-3}), since all the estimations are minimum estimations.

Now, let us estimate the wave energy flux density of the detected kink MHD waves. Using eqs. (a4) and (a5), the time-averaged wave energy flux ($\langle E_k \rangle$) carried by the fast kink MHD wave can be estimated in the moving thread of the quiescent prominence, as refs. [29, 49, 53].

$$\langle E_k \rangle \approx \frac{1}{4} c_{\rm ph} \left(\rho\, v^2 + \frac{b^2}{\mu_0} \right), \tag{a4}$$

$$b \approx B \frac{2\pi}{\lambda} A_m. \tag{a5}$$

Here, v is the velocity amplitude of the transverse oscillation, b is the Lagrangian perturbation of the magnetic field. We want to state that eq. (a5) is an estimation with the Lagrangian displacement vector, according to eq. (4) in ref. [53].